Cell Cycle-Regulated Transcription of CENP-A by the MBF Complex Ensures Optimal Level of CENP-A for Centromere Formation

David Aristizabal-Corrales, Jinpu Yang, and Fei Li[1]

Department of Biology, New York University, 1009 Silver Center, New York 10003

ABSTRACT The centromere plays an essential role in chromosome segregation. In most eukaryotes, centromeres are epigenetically defined by the conserved histone H3 variant CENP-A. Proper centromere assembly is dependent upon the tight regulation of CENP-A level. Cell cycle regulation of CENP-A transcription appears to be a universal feature across eukaryotes, but the molecular mechanism underlying the temporal control of CENP-A transcription and how such regulation contributes to centromere function remains elusive. CENP-A in fission yeast has been shown to be transcribed before S phase. Using various synchronization methods, we confirmed that CENP-A transcription occurs at G1, leading to an almost twofold increase of the protein during S phase. Through a genetic screen, we identified the MBF (MluI box-binding factors) complex as a key regulator of temporal control of CENP-A transcription. The periodic transcription of CENP-A is lost in MBF mutants, resulting in CENP-A mislocalization and chromosome segregation defects. We identified the MCB (MluI cell cycle box) motif in the CENP-A promoter, and further showed that the MBF complex binds to the motif to restrict CENP-A transcription to G1. Mutations of the MCB motif cause constitutive CENP-A expression and deleterious effects on cell survival. Using promoters driving transcription to different cell cycle stages, we found that timing of CENP-A transcription is dispensable for its centromeric localization. Our data instead indicate that cell cycle-regulated CENP-A transcription is a key step to ensure that a proper amount of CENP-A is generated across generations. This study provides mechanistic insights into the regulation of cell cycle-dependent CENP-A transcription, as well as its importance on centromere function.

KEYWORDS centromere; CENP-A; cell cycle transcriptional control; the MBF complex; *Schizosaccharomyces pombe*

THE centromere is the special chromosomal locus where the kinetochore is assembled. The kinetochore interacts with the spindle microtubules to mediate equal segregation of sister chromatin to daughter cells during mitosis and meiosis (McKinley and Cheeseman 2016). In most eukaryotes, centromeres are epigenetically defined by a conserved histone H3 variant, CENP-A. CENP-A partially replaces the canonical histone H3 in centromeres and promotes the assembly of kinetochores (Black *et al.* 2007; Allshire and Karpen 2008). Proper centromere assembly is dependent upon the tight regulation of CENP-A levels. Overexpression of CENP-A in many organisms causes misincorporation of CENP-A into

noncentromeric regions, leading to chromosome missegregation and growth defects (Heun *et al.* 2006; Olszak *et al.* 2011; Choi *et al.* 2012; Castillo *et al.* 2013; Gonzalez *et al.* 2014; Dong *et al.* 2016; Shrestha *et al.* 2017). CENP-A overexpression has been observed in a number of cancers, which might contribute to chromosome instability (Tomonaga *et al.* 2003; Li *et al.* 2007; Amato *et al.* 2009; Scott and Sullivan 2014; Zhang *et al.* 2016).

During replication, parental CENP-A appears to be partitioned equally between sister chromatids to be incorporated into two daughter centromeres (Jansen *et al.* 2007; Schuh *et al.* 2007; Black and Cleveland 2011), But the timing of the loading of newly synthesized CENP-A varies among different organisms. In plants and fission yeast *Schizosaccharomyces pombe*, new CENP-A is loaded into centromeres during G2 (Lermontova *et al.* 2006; Takayama *et al.* 2008; Lando *et al.* 2012; Gonzalez *et al.* 2013), whereas the loading of CENP-A in humans, *Drosophila*, and budding yeast occurs in G1, mitosis, and S phase, respectively (Pearson *et al.* 2004; Jansen

et al. 2007; Mellone et al. 2011; Wisniewski et al. 2014). CENP-A transcription is also cell cycle-regulated. While CENP-A is transcribed in the G2/M window in humans, it occurs in G1/S phase in fission yeast. It appears that CENP-A transcription is generally uncoupled from canonical histone transcription (Shelby et al. 1997, 2000; Takahashi et al. 2000; Whitfield et al. 2002; Bar-Joseph et al. 2008; Rattray and Muller 2012; Grant et al. 2013). However, the molecular basis underlying cell cycle-regulated CENP-A transcription remain little known.

Interestingly, CENP-A expressed under the control of the H3 promoter fails to localize to the centromere and shows diffuse localization in the nucleus of human cells. This evidence prompted some to suggest that the timing of CENP-A expression, which is uncoupled from histone transcription during S phase, plays an important role in centromere targeting (Shelby et al. 1997). However, this hypothesis has not been formally tested. This study aims to unveil the mechanism behind CENP-A transcriptional regulation during the cell cycle, and its impact on CENP-A localization and function in fission yeast.

Here, we confirmed that CENP-A/Cnp1 in fission yeast is transcribed at G1 phase using multiple synchronization methods. We identified the MBF (MluI box-binding factors) complex as a key regulator of cell cycle-dependent CENP-A transcription. The MBF complex binds to the MCB (MluI cell cycle box) motif in the CENP-A promoter to restrict its transcription to G1 phase. However, using promoters driving transcription at different stages of the cell cycle, we found that timing of CENP-A transcription is dispensable for its centromere localization. Instead, our data indicate that cell cycle regulation of CENP-A transcription is a key step to ensure the proper of CENP-A generated across generations.

Materials and Methods

Strains, media, and genetic analysis

Fission yeast strains used in this study are listed in Supplemental Material, Table S1. Standard media and genetic analysis for fission yeast were used (Moreno et al. 1991). The mutant screen will be described in detail elsewhere (J. Yang and F. Li, unpublished data). Briefly, mutants from the Bioneer haploid deletion library were crossed with wild-type (WT) cells carrying Cnp1-GFP using a Rotor-HDA pinning robot (Singer Instruments). The resulting mutant cells carrying Cnp1-GFP were visually examined by fluorescence microscopy.

Western blot analysis

Western blot assays were performed as described with a few modifications (Huang et al. 2017). Briefly, cell extracts from exponentially growing cells were collected. Protein extracts were denatured in loading buffer (SDS 2%, glycerol 10%, Tris-Cl 60 mM, and 0.002% bromophenol blue), separated on 12% SDS-polyacrylamide gels, and transferred onto PVDF

membranes. Membranes were blotted with primary anti-GFP (sc-9996; Santacruz) or α-tubulin (ab6160; Abcam) antibodies. Image J software was used for band quantification.

Cell synchronization

Centrifugal elutriations were conducted as previously described (Tormos-Pérez et al. 2016). Briefly, cells grown to the log phase at ~23°, OD ~1 at 600 nm, were collected and loaded into a Beckman J6 centrifuge with a JE−5.0 elutriation rotor. The smallest cells were eluted and were incubated at ~23° for 6 hr. Samples for cell fixation (to determine septation index), RNA and protein extraction were collected every 15 min. Septation index was determined after fixing cells in 70% ethanol and staining with calcofluor (Sigma [Sigma Chemical], St. Louis, MO) and DAPI. For the cdc10 block-release experiments, cdc10-129 cells were grown at 25° to log phase and then shifted to 36° for 3.5 hr. Samples for RNA extraction were collected before and after the shift. For hydroxyurea (Sigma) treatment, exponentially growing cells were incubated in 10 mM hydroxyurea for 4 hr. Samples for RNA extraction were collected before and after hydroxyurea treatment.

Quantitative RT- PCR

RT-PCR assays were performed as previously described (He et al. 2017). Briefly, samples were homogenized using glass beads and a tube beater. Total RNA was purified using TRIzol. After treatment with RQ1 DNAse (Promega, Madison, WI), RNA was precipitated again with ethanol and used for cDNA synthesis with a PrimeScript RT Reagent Kit (Takara, Clontech). Next, 25 ng of cDNA were used for each quantitative PCR (qPCR) reaction using 2× SYBR Green qPCR Master Mix (Bimake). adh1 was used as a loading control. Fold change comparing to the corresponding experimental controls was calculated following the standard ΔΔCt method. Primers used for qPCR are listed in Table S2.

ChIP-qPCR

Chromatin immunoprecipitation (ChIP) assays were performed as described previously (Kong et al. 2016). Briefly, cells were grown to log phase at 30° and cross-linked by treatment with 1% formaldehyde. Immunoprecipitation was performed with protein A agarose (KPL) and anti-GFP antibody (ab290; Abcam). Next, 2 μl of ChIP or whole-cell extract samples were analyzed by qPCR using primers targeting hht1, cdc18, and cnp1 promoter regions. act1 was used as an internal control.

In situ chromatin-binding assay

In situ chromatin-binding assays were performed as described (Yang and Li 2018). Briefly, log-phase cells were collected and incubated in ZM buffer for 30 min. Cells were then washed twice with STOP buffer. Cells were resuspended with EB (extraction buffer) buffer ± 1% Triton X-100 at room temperature for 7 min, followed by fixation with 3.7% formaldehyde and 10% methanol.

Microscopy

Live or DAPI-stained fixed cells were imaged using a Delta Vision System (Applied Precision, Issaquah, WA) coupled to an Olympus IX71 microscope. Images were taken as z-stacks of 0.2-μm increments with an oil immersion objective (×100), and deconvolved using SoftWoRX2.50 software (Applied Precision).

Thiabendazole sensitivity assay

Serial dilutions (10-fold) of log phase cells were spotted on plates with 15 μg/ml thiabendazole (TBZ) (Sigma). Cell growth was estimated by taking pictures after incubating the plates for 72 and 92 hr at 30°.

Data availability

Strains and plasmids are available upon request. The authors affirm that all data necessary for confirming the conclusions of the article are present within the article, figures, and tables. Supplemental material available at Figshare: https://doi.org/10.25386/genetics.7268501.

Results

Expression level of CENP-A is cell cycle-regulated in fission yeast

Using cells synchronized by a block-and-release approach in a *cdc25-22* temperature-sensitive (*ts*) background, a previous report showed that the transcription of *cnp1* appeared to be cell cycle-regulated in fission yeast. The mRNA is expressed around G1/S transition, peaking just before the onset of histone H3 transcription (Takahashi *et al.* 2000). To confirm the pattern of *cnp1* expression, we synchronized WT cells at G2 phase by centrifugal elutriation and followed the expression of *cnp1* mRNA from its native locus for 5.5 hr of synchronous growth using quantitative (q)RT-PCR. In fission yeast, the peak of septum-containing cells marks the time of the S phase. We found that most of the cells (~80%) underwent the S phase 150 min after elutriation, based on the septation index. Accordingly, the peak of septation matches with the peak of expression of the histone H3 (*hht1* gene) as histones are highly expressed during S phase (Figure 1A). Consistent with the previous report (Takahashi *et al.* 2000), *cnp1* mRNA peaks before the transcription of histone H3, ~120 min after elutriation, showing an approximately twofold increase. This pattern of expression coincides with the expression of *cdc18*, a well-known cell cycle-regulated gene expressed specifically in G1 phase (Figure 1A). We also observed the same transcription pattern in cells expressing Cnp1-GFP under its native promoter integrated next to the *ade6* gene (Figure S1).

To test whether the observed mRNA regulation has an impact on the protein level, we tagged Cnp1 with GFP under its native promoter and checked the levels of protein by western blotting using samples from the same synchronization method (Figure 1B). Cnp1-GFP protein increases approximately twofold at 165-min postelutriation. This result

indicates that the mRNA increase in G1 results in augmentation of the Cnp1 protein level in S phase. Since Cnp1 in fission yeast has been suggested to be assembled into chromatin, mainly in G2 (Takayama *et al.* 2008; Lando *et al.* 2012), the timing of the increase of the Cnp1 protein level seem to be coordinated to provide the protein necessary for the next round of assembly.

We also checked the *cnp1* mRNA levels in cells synchronized at G1 phase using a temperature-sensitive allele of the *cdc10* gene, as well as in cells treated with hydroxyurea, which arrests cells at the beginning of S phase. *cnp1* mRNA is increased in both G1 and S phase-arrested cells, whereas histone H3 transcripts are increased in S but not in G1-arrested cells (Figure S2). Other known G1 phase-regulated genes such as *cdc18* and *cdc22* show the same pattern as *cnp1* (Figure S2). These results confirm that *cnp1* is cell cycle-regulated at the mRNA and protein levels, and that its pattern of expression is uncoupled from H3 expression.

MBF complex mutants exhibit an abnormal CENP-A distribution pattern and chromosome missegregation

We recently initiated a visual genetic screen to identify factors involved in the regulation of CENP-A distribution using Cnp1-GFP as a visual marker. Three centromeres are clustered underneath the nuclear envelope near the spindle pole body in *S. pombe* WT interphase cells. Therefore, a single Cnp1-GFP focus is observed in the WT cells expressing Cnp1-GFP (Funabiki *et al.* 1993; He *et al.* 2016). Through the visual screen, we identified that three mutants, *nrm1Δ*, *yox1Δ*, and *res2Δ*, showed abnormal CENP-A distribution patterns (Figure 2A). In these mutants, Cnp1-GFP at centromeres tends to be brighter and also gives a high nucleoplasmic signal (Figure 2A), suggesting an increase in Cnp1-GFP levels. Interestingly, the increased nuclear signal is only partially washed away by Triton X-100 treatment, indicating that the mislocalized Cnp1-GFP stably associates with chromatin regions other than centromeres (Figure S3). Genes corresponding to these mutants, *res2*, *nrm1*, and *yox1*, are all from the conserved MBF transcription factor complex. The MBF complex regulates the transcription of genes required for DNA replication during the G1/S transition of the cell cycle (Bahler 2005; Bertoli *et al.* 2013; Haase and Wittenberg 2014) (Figure 2B), which is the time when *cnp1* mRNA levels peaks (Figure 1A). Res2, a DNA-binding protein, together with Res1 and Cdc10, forms the core of the MBF complex, and is involved in both activation and repression of the transcriptional activity (Ayté *et al.* 1995, 2001; Baum *et al.* 1997; Zhu *et al.* 1997; Whitehall *et al.* 1999; Dutta *et al.* 2008). Nrm1 and Yox1 are negative regulatory components of the MBF complex (Aligianni *et al.* 2009; Purtill *et al.* 2011).

It has been shown that increased Cnp1 levels can result in Cnp1 mislocalization, which affects chromosome segregation (Gonzalez *et al.* 2014). Using DAPI staining, we observed that the MBF repressor mutant cells displayed lagging chromosomes, chromosome bridges, and also unequal nuclei segregation during mitosis (Figure 2C and Figure S4). Around
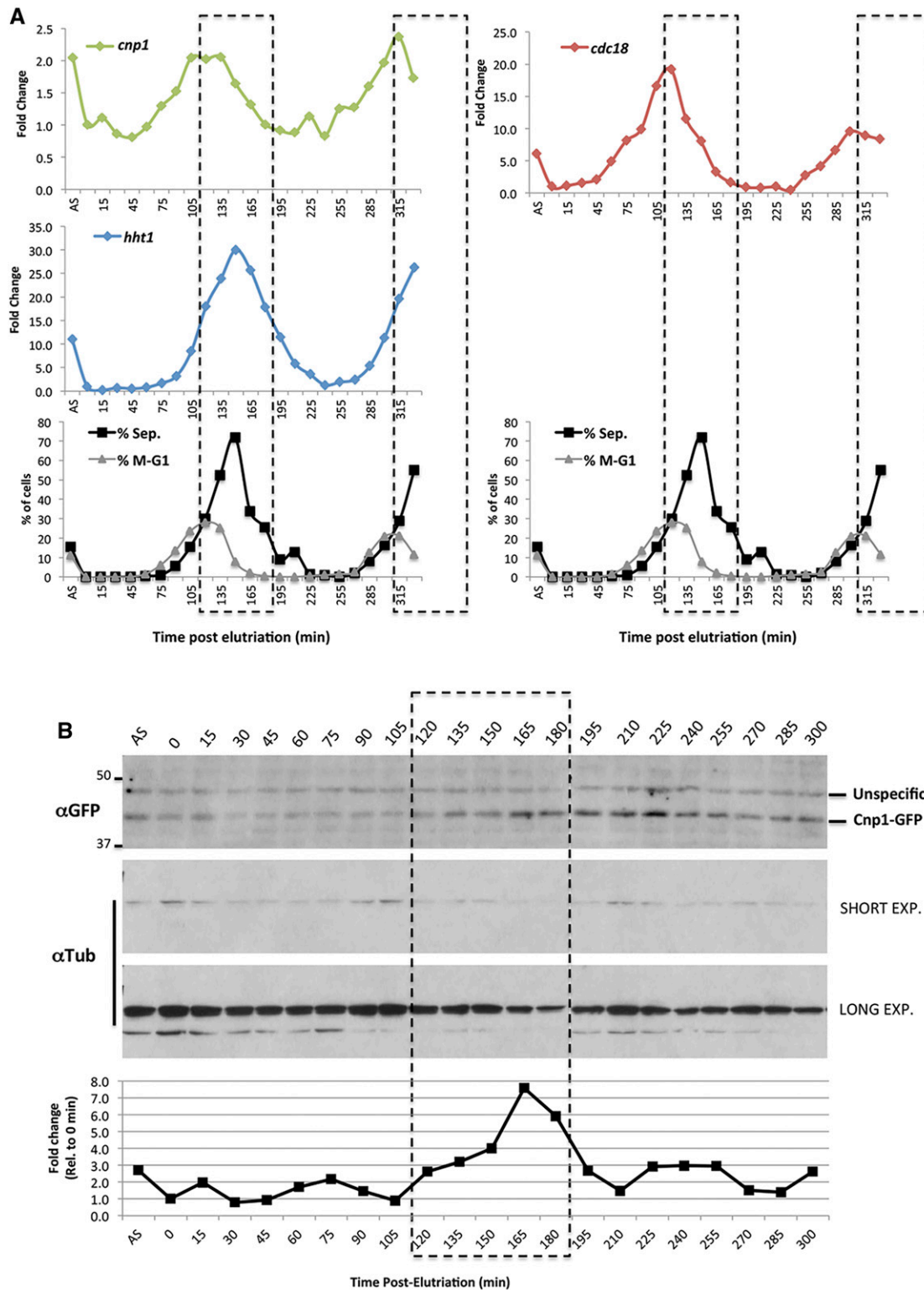
Figure 1 Cell cycle-regulated expression of Cnp1. (A) Quantitative RT-PCR analysis of *cnp1* expression in wild-type cells after synchronization by elutriation. Cells were synchronized in G2 by centrifugal elutriation and grown for 5 hr. Total mRNA was prepared at the indicated times postsynchronization. AS indicates a sample from the asynchronous population before elutriation. Upper panels show fold change of the indicated gene RNAs compared to a sample at 0 min. Lower panel show the percentage of septated cells and cells undergoing mitosis/G1 phase scored by DAPI and calcofluor staining at the indicated times for the same experiment. Dotted line indicates the S phase window determined by the septation index. (B) Western blot analysis of Cnp1 expression in cells after release from synchronization. Cell lysates were prepared from the same experiment described above, and processed for western blot analysis using antibodies specific for GFP and tubulin (as a loading control). Lower graph shows quantification of the Cnp1-GFP bands normalized to tubulin at each time point. Short and long time exposures (exp.) are shown for tubulin blotting.
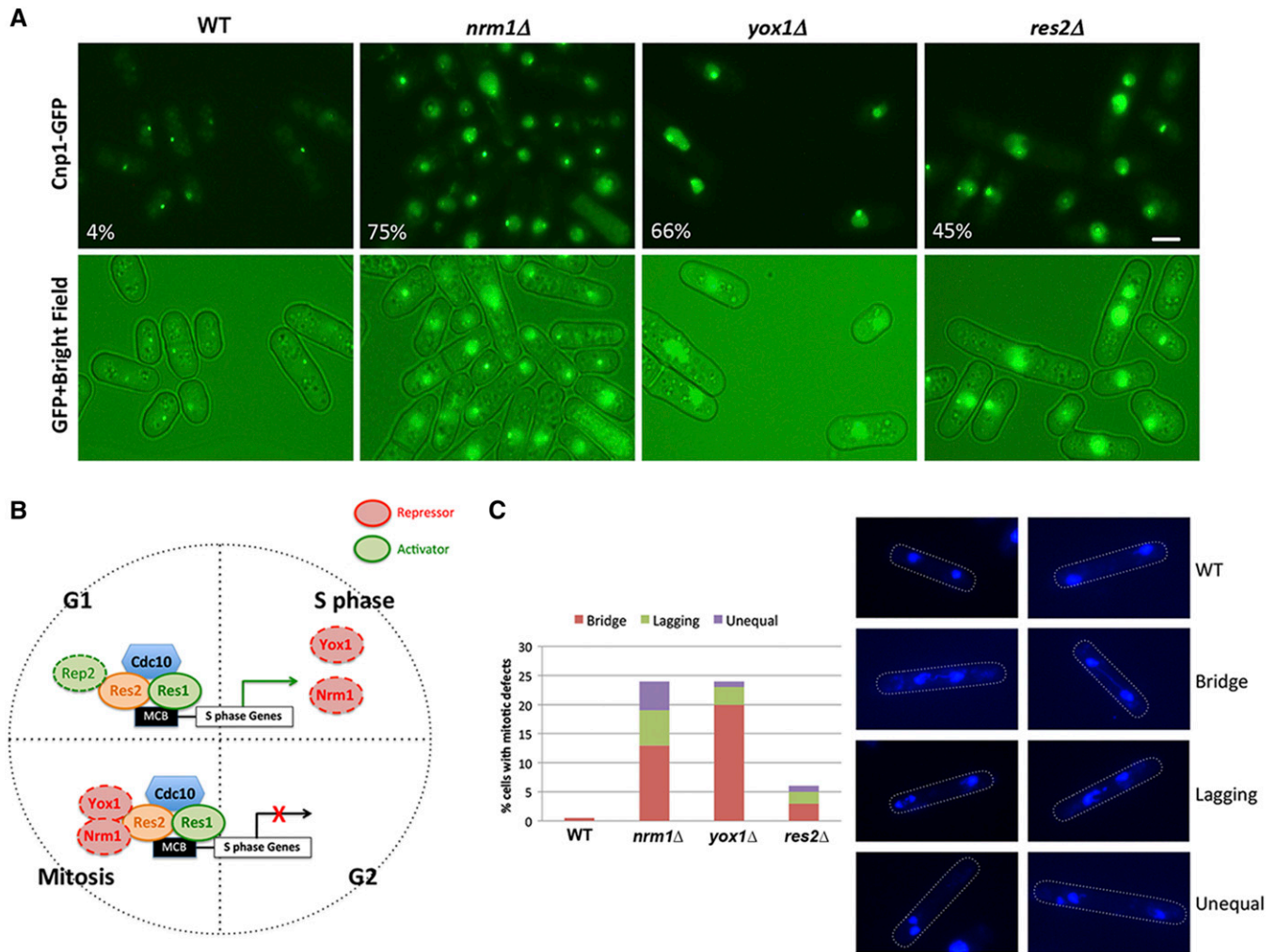
Figure 2 The MBF complex mutants show defects in CENP-A distribution and chromosome segregation. (A) Images of Cnp1-GFP localization in *nrm1Δ*, *yox1Δ*, and *res2Δ* mutants obtained by imaging live cells carrying the endogenous copy of *cnp1* tagged with GFP. Bar, 2 μm. (B) Scheme showing the regulation of G1/S-expressed genes by the MBF complex. The core of the complex consists of Cdc10, Res1, and Res2, which bind to promoters containing MBF-binding motifs (MCB boxes). Rep2 normally acts as a cofactor for transcriptional activation. At the G1/S transition, the complex promotes the transcription of genes required for S phase, including Nrm1 and Yox1. The proteins coded by these two genes act as repressors of the MBF complex by binding to Res2 and limiting its transcriptional activity. This mechanism sets a negative feedback loop that restricts the activation of MBF targets during the rest of the cell cycle. (C) Overexpression of Cnp1-GFP causes chromosome segregation defects in mitotic cells. Right panel shows DAPI-staining images of *nrm1Δ*, *yox1Δ*, and *res2Δ* fixed cells. The percentage of mitotic cells showing bridge, lagging, or unequal chromosomes is indicated in the left panel. MBF, MluI box-binding factors; MCB, MluI cell cycle box; WT, wild-type.

25% of *nrm1Δ* and *yox1Δ* mutant cells displayed mitotic defects, while *res2Δ* mutants showed a relatively mild defect.

Cell cycle-regulated CENP-A transcription depends on the MBF complex

The pattern of *cnp1* expression during the cell cycle and the phenotype observed in the MBF regulator mutants suggest that the MBF complex may be involved in the regulation of *cnp1* expression. Accordingly, an increase in both *cnp1* mRNA and protein levels was observed in asynchronous populations of *nrm1*, *yox1*, and *res2* mutants (Figure 3, A and B). Deletion of *nrm1* or *yox1* resulted in a ~5–6-fold increase in *cnp1* mRNA levels, whereas *res2* deletion led to a more modest twofold increase (Figure 3A). The magnitude of the observed defects (Figure 2, A and C) is correlated with the increase in *cnp1* levels observed in these mutants (Figure 3, A and B).

A similar increase was observed in the *cdc18* mRNA, which is a known target of the MBF complex (Kelly *et al.* 1993). We noticed that *H3* (*hht1*) and *spd1* genes, which are expressed in the S and G2 phases, respectively, and mediated by different transcription complexes, also showed a slight increase in MBF mutants (Figure 3A). This suggests that mutation of these genes may disturb the cell cycle program of the cells, which is not unexpected since the MBF complex regulates the G1/S transition. Interestingly, mutation of *rep2*, which is required for the transcriptional activation of other MBF targets (Nakashima *et al.* 1995), does not cause a significant change in *cnp1* levels (Figure 3A).
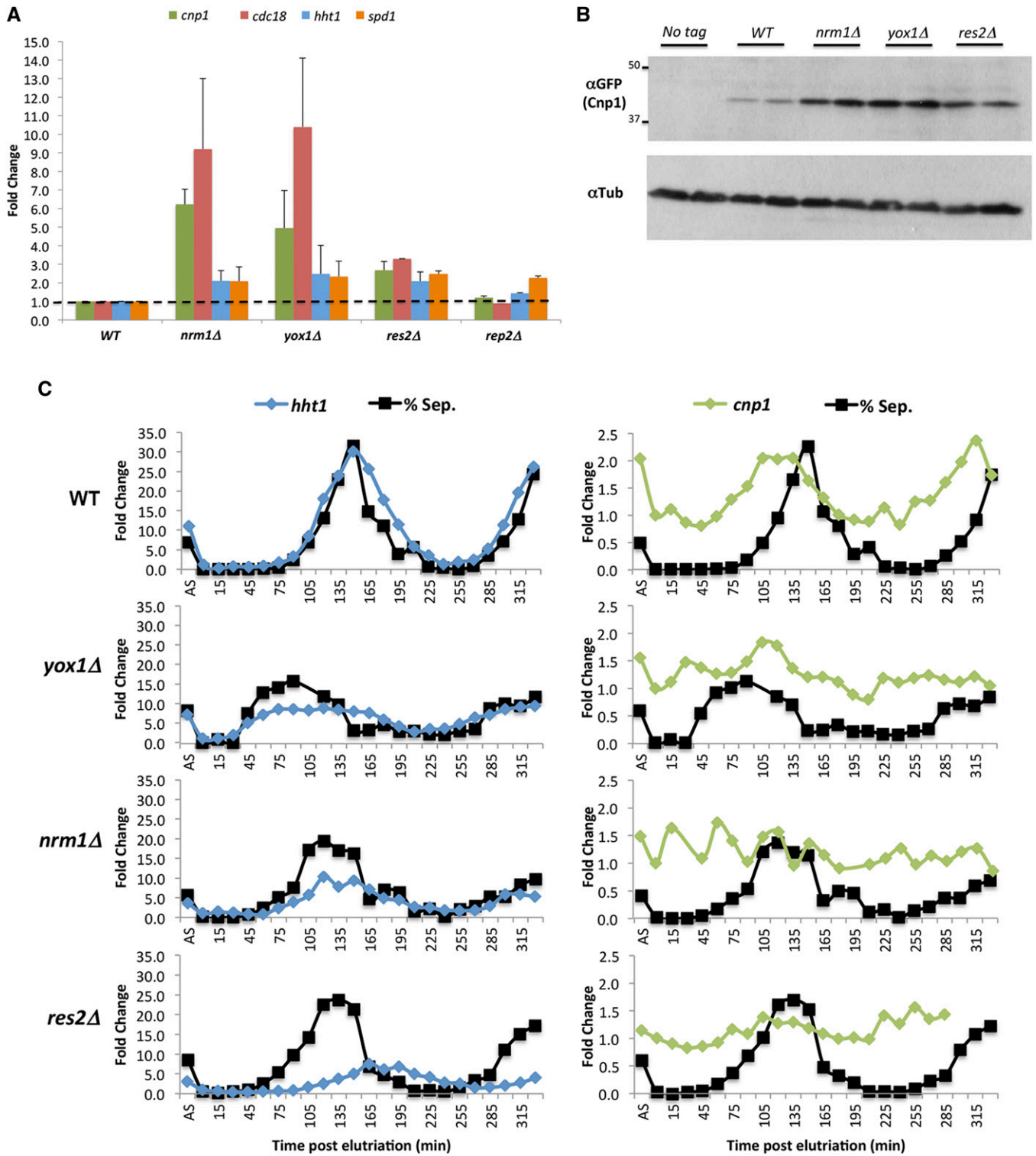
Figure 3 The MBF complex is required for cell cycle-regulated CENP-A transcription. (A) Quantitative RT-PCR analysis of *cnp1* RNA expression in *nrm1Δ*, *yox1Δ*, *res2Δ*, and *rep2Δ* cells. Total mRNA was prepared from asynchronous cells. Fold change for the indicated genes (different colored bars) was calculated compared to WT cells. (B) Western blot analysis of Cnp1-GFP levels for the MBF complex repressors mutants. Tubulin was used as a loading control. First two lines show blotting for a WT strain with no GFP tag on Cnp1 as control of antibody specificity. (C) Quantitative RT-PCR analysis of *cnp1* mRNA levels throughout the cell cycle using synchronized *nrm1Δ*, *yox1Δ*, and *res2Δ* cells. Cells were synchronized by elutriation and grown for 5.5 hr. Total RNA was prepared and septation index scored every 15 min. Each graph shows the fold change for *hht1* (left panels) or *cnp1* (right panels) RNAs at the indicated times compared to a 0-min sample. Black curve on each graph shows the septation index of the corresponding cell population as reference. AS: asynchronous culture; MBF, MluI box-binding factors; WT, wild-type.

To further investigate how the MBF mutants affect the cell cycle regulation of *cnp1*, we examined *cnp1* mRNA levels throughout the cell cycle using synchronized *nrm1Δ*, *yox1Δ*, and *res2Δ* mutant cells. We found that, in contrast to WT cells, the mutants do not show a clear peak of *cnp1* expression right before septation (Figure 3C). However, we also noticed that these mutants do not synchronize as well as WT cells, as evidenced by the percentage of cells obtained at the peak of septation (∼70% in WT *vs.* 35, 45, and 50% in *nrm1*, *yox1*, and *res2*, respectively) (Figure 3C). In addition, the fold change and timing of H3 expression also seem to be affected. Histone H3 levels are regulated by an MBF target, *ams2* (Rustici *et al.* 2004; Takayama and Takahashi 2007), so deletion of MBF repressors is expected to indirectly impact H3 levels. MBF also regulates a set of genes required for S phase, so the overall cell cycle program is also expected to be affected. Therefore, the observed defect on *cnp1* mRNA in asynchronous cells is probably resulting from a combined effect of the direct disruption of *cnp1* transcription control by MBF and an indirect effect caused by a cell cycle distribution defect on the MBF mutants. Overall, these results show that mutation of MBF repressor genes leads to the deregulation and increase of *cnp1* levels, and mitotic defects.

The MBF complex binds to an MCB motif in the cnp1 promoter

To investigate how the MBF complex regulates *cnp1* transcription, we tested the binding of several MBF factors to the *cnp1* promoter by ChIP. The MBF complex is known to target the promoters of genes such as *cdc18* and *cdc22*. The promoter motifs bound by the MBF complex are called MCB motifs (Lowndes *et al.* 1992). Our *in silico* analysis revealed that the *cnp1* promoter contains two putative MCB boxes at −110 and −478-bp upstream of the start codon, which we named MCB1 and MCB2, respectively (Figure 4A). ChIP analysis showed that Nrm1, Yox1, and Res2 bind to the *cnp1* promoter (Figure 4B). Nrm1 and Yox1 are known to form a dimer that suppresses the transcriptional activity of the MBF complex outside of G1 by interacting with Res2 (de Bruin *et al.* 2006; Aligianni *et al.* 2009; Caetano *et al.* 2011). Consistent with these studies, we found that the *nrm1Δ yox1Δ* double mutants show roughly the same elevated level of *cnp1* mRNA as the single mutants (Figure 4C). The observation confirmed that Nrm1 and Yox1 are functionally dependent on each other in suppressing *cnp1* expression. Furthermore, the *nrm1Δ res2Δ* and *yox1Δ res2Δ* double mutants display the same *cnp1* mRNA level as the *res2Δ* single mutant (Figure 4C), suggesting that Nrm1 and Yox1 suppress *cnp1* levels by interacting with Res2.

The MBF complex restricts CENP-A transcription to G1 phase

To probe the functionality of the two putative MCB boxes in the *cnp1* promoter, we made single (ΔMCB1 and ΔMCB2) and double deletions of the boxes (ΔMCB 1+2) (Figure 5A). We also mutagenized the core CG nucleotides in each

MCB box into TA (MCB ta 1 and MCB ta 2) as an alternative way to disturb the putative binding of MBF proteins (Figure 5A). The *cnp1* gene containing these mutations was tagged with GFP and introduced at the *ade6* site by homologous recombination. Our qRT-PCR analysis showed that mutation or deletion of the MCB1 box (located −110 bp from the start codon) results in a four-to-fivefold increase in the *cnp1* mRNA level (Figure 5B). Mutation of the MCB2 box (−478 bp from the start codon) does not have any detectable effect on the mRNA levels of *cnp1* and therefore this box was considered to not be functional. The increase in mRNA levels in the MCB1 mutant also results in an increase in protein levels (Figure 5C). Interestingly, mutation of the MCB1 mimics the increase in *cnp1* levels observed in the MBF repressor mutants (*nrm1*, *yox1*, and *res2*). Even though most of the MCB1 mutant cells show a single Cnp1-GFP focus corresponding to its normal centromeric localization, we observed several differences when comparing with *cnp1-gfp* under the control of the WT promoter. The MCB1 mutant cells display brighter centromeric foci with an average increase of twofold in signal intensity, suggesting an increase in the amount of Cnp1 assembled at the centromere (Figure 5D and Figure S5). Additionally, we observed that some of these mutant cells show either diffuse or multifoci Cnp1-GFP localization (Figure 5D). These results suggest that mutation of the MCB1 box leads to CENP-A overexpression and defective localization.

Based on these observations, we hypothesized that an intact MCB1 box is required for the binding of the MBF repressors to the *cnp1* promoter to restrict the expression of *cnp1*. To test this idea, we checked the expression of the *cnp1-gfp* reporter gene (extra copy, inserted at the *ade6* site) with a WT or MCB1 mutant promoter in the background of the MBF repressor mutants (Figure 6A). Mutation of the MBF repressors causes an increase in the expression of the *cnp1-gfp* reporter gene with the WT promoter (three-, five-, and twofold for *nrm1Δ*, *yox1Δ*, and *res2Δ*, respectively). A similar increase was observed for the *cnp1* endogenous copy. However, in cells carrying *cnp1-gfp* controlled by the promoter with MCB1 deletion, mutation of *nrm1* and *yox1* caused just a modest increase of 1.5- and 1.7-fold change, respectively, and no increase was observed in *res2* mutants. This indicates that the MBF repressors require the MCB1 box to fully repress *cnp1* levels.

To further test the functional consequences of disrupting the MCB1 box, we mutated this box in the *cnp1* endogenous gene. This caused disturbed expression of *cnp1* during the cell cycle in a synchronized cell population (Figure 6B), with *cnp1* RNA levels being induced well in advance of the G1/S transition. This suggests that the MCB1 box is required to restrict *cnp1* expression to the G1 phase. We also noticed that cells carrying the MCB1 deletion showed an ∼30-min delay in the cell cycle with most of the cells undergoing S phase (*hht1* RNA peak) ∼165 min postelutriation, compared to 135 min in WT cells. As observed with the reporter gene, mutation or deletion of the endogenous MCB1 box resulted in an increase in the levels of *cnp1* (Figure S6). The magnitude
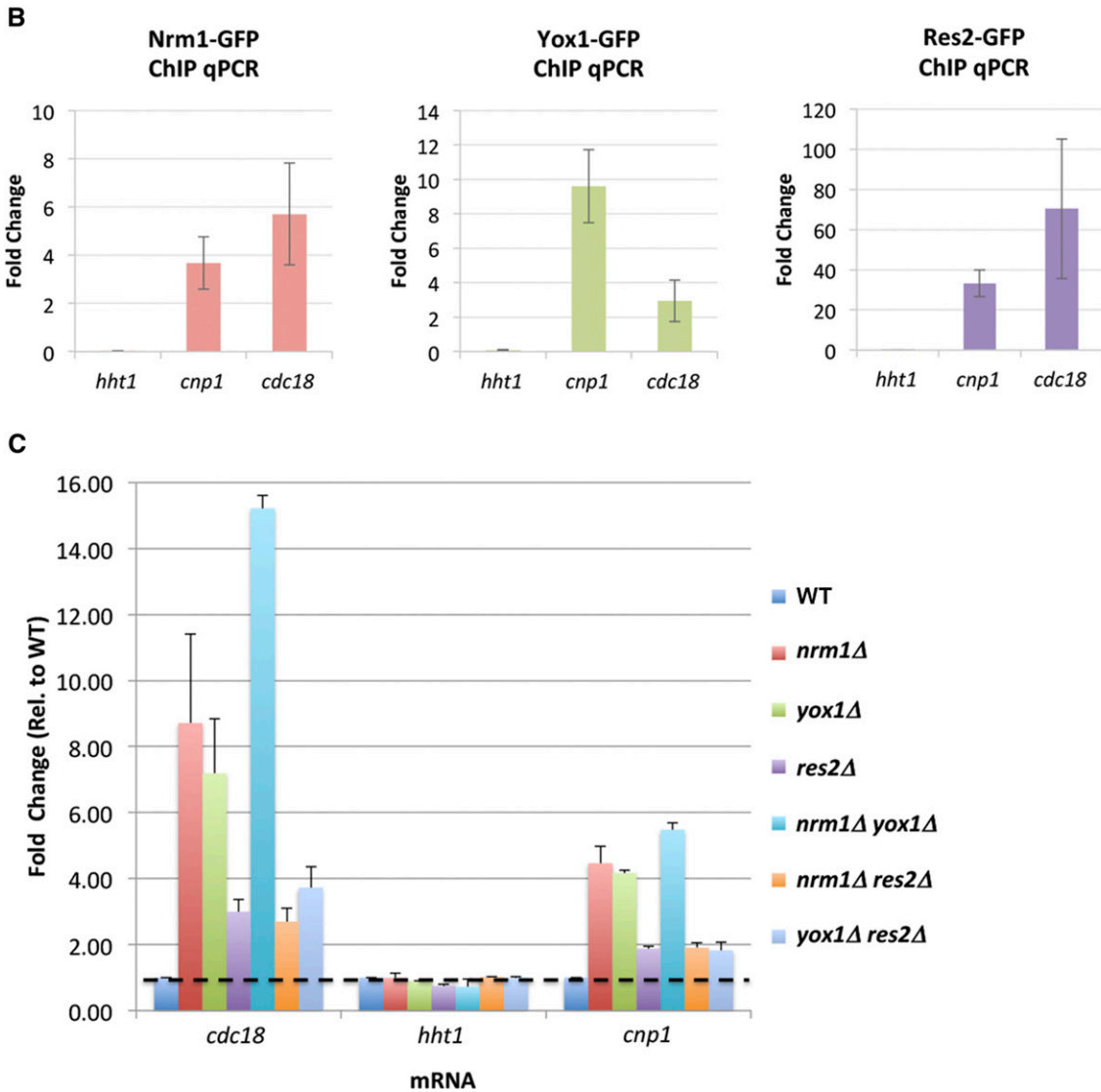
Figure 4 The MBF complex binds to the MCB motif on the *cnp1* promoter. (A) Map of putative MCB boxes in the *cnp1* promoter. MCB1 and MCB2 coordinates are indicated. ATG in bold letters marks the Cnp1 start codon. (B) Nrm1, Yox1, and Res2 bind to the promoter region of *cnp1*. ChIP assays were performed using WT cells carrying Nrm1-GFP, Yox1-GFP, or Res2-GFP using primers specific for the promoter region of *cnp1*, *hht1*, and *cdc18*. *hht1* and *cdc18* were used as negative and positive controls, respectively (C) Quantitative RT-PCR analysis of *cnp1* mRNA levels in cells with single or double mutations of the MBF complex. Fold change compared to WT cells was calculated for *cdc18*, *hht1*, and *cnp1* RNAs. Bars on different colors correspond to the fold change in the indicated mutants. ChIP, chromatin immunoprecipitation; MBF, MluI box-binding factors; MCB, MluI cell cycle box; qPCR, quantitative PCR; WT, wild-type.
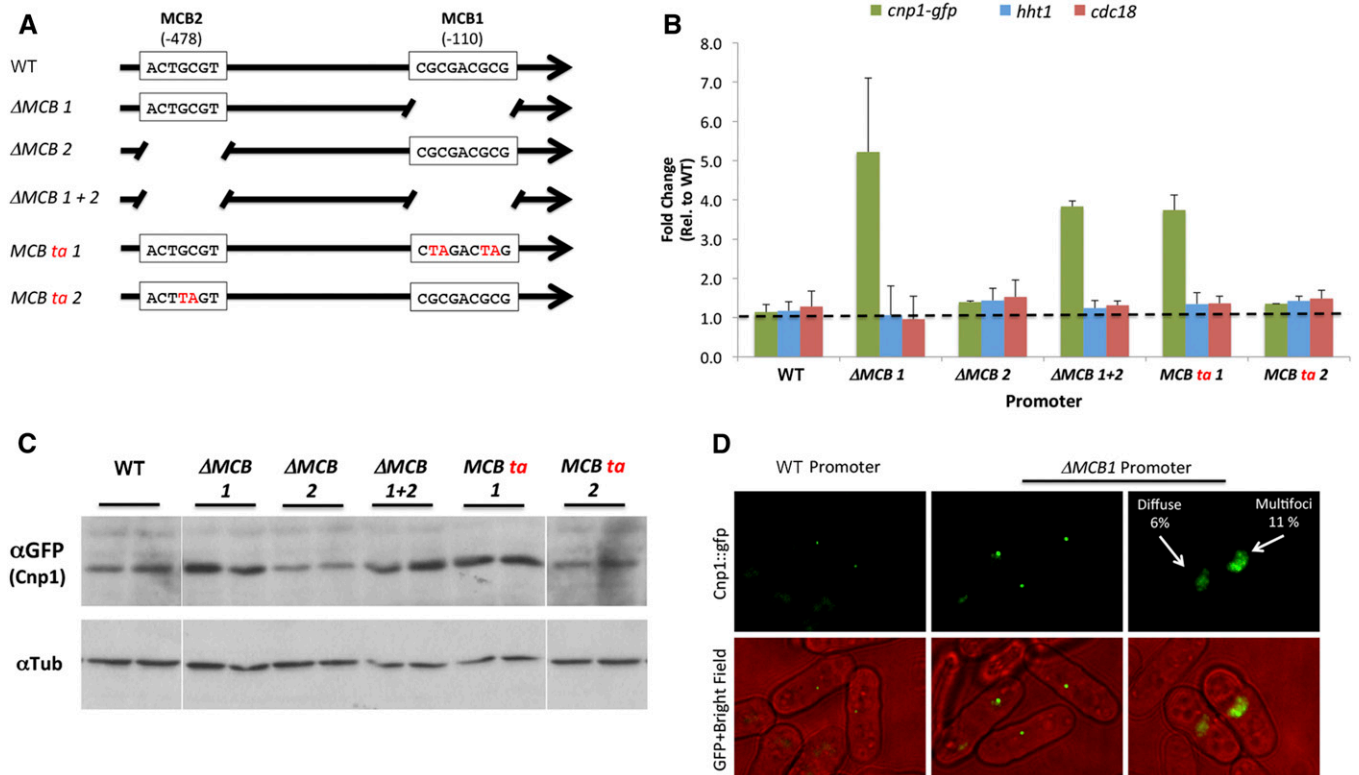
Figure 5 Cell cycle-regulated expression of Cnp1 is abnormal when the MCB1 box is mutated. (A) Schematic representation of the *cnp1* promoter mutant constructs. Predicted MCB box 1 or 2 was disrupted by either deletion or substitution of the core GC bases to TA. (B) Quantitative RT-PCR analysis of *cnp1-gfp*, *hht1*, and *cdc18* RNAs in cells carrying *cnp1-gfp* under control of a promoter with the indicated mutations in the MCB boxes. *hht1* and *cdc18* were used as negative controls since their expression should not be affected by mutations in the *cnp1* promoter (C) Western blot analysis of Cnp1-GFP level from the same experiment shown in (B). Tubulin was used as a loading control. (D) Images of Cnp1-GFP in live cells carrying the *WT cnp1* promoter or ΔMCB1 promoter. Percentages of cells showing the indicated abnormal Cnp1 localization are indicated. MCB, MluI cell cycle box; WT, wild-type.

of this increase was variable among different clones containing the same MCB1 mutation. When we subjected these cells to mitotic stress by treatment with the microtubule polymerization inhibitor TBZ, we observed a slight but consistent decrease in growth of the cells (Figure 6C). This was correlated with the presence of bridged and lagging chromosomes in these mutants (Figure 6D). The cells showing slower growth on TBZ and more mitotic errors were the ones expressing higher levels of *cnp1* mRNA (Figure S6), suggesting that tight regulation of *cnp1* levels is required to avoid mitotic defects. Together, these results demonstrate that the MBF repressor genes bind to the *cnp1* promoter via the MCB1 box to restrict its expression, and avoid *cnp1* overexpression and chromosome missegregation.

The timing of CENP-A expression is dispensable for its targeting to centromeres

We next tested the previously suggested hypothesis that the timing of CENP-A transcription contributes to the proper targeting of *cnp1* (Shelby *et al.* 1997). This hypothesis was proposed based on the observation that forcing expression of CENP-A in S phase using the histone H3 promoter leads to the mislocalization of the protein in human cells (Shelby *et al.*

1997). To determine whether the timing of CENP-A expression is important for its targeting to centromeres, we expressed a *cnp1-gfp* reporter gene under the control of a variety of promoters that drive expression at different stages of the cell cycle (Figure 7A). They include promoters from histone H3 (*hht1*), *spd1*, *plo1*, *spo12*, *cdc15*, and *cdc18*, which direct transcription at S, G2, late G2, mitosis, mitosis/G1, and G1 phase, respectively. *cnp1-gfp* mRNA and protein levels produced by the different promoters were analyzed (Figure 7, B and C). We also analyzed the localization of Cnp1-GFP expressed from different promoters (Figure 7D). In agreement with the previous report in human cells (Shelby *et al.* 1997), expression of *cnp1-gfp* under control of the histone H3 promoter led to multiple foci of Cnp1-GFP with strong signal in nuclei, suggesting ectopic localization of the protein. Multiple Cnp1-GFP foci were also found in cells expressing Cnp1-GFP under the *spd1*, *spo12*, and *cdc18* promoters. However, most cells expressing Cnp1-GFP driven from the *plo1* and *cdc15* promoter contain a single Cnp1-GFP focus, though the c*dc15* promoter results in a brighter Cnp1-GFP spot. Accordingly, we found that Cnp1-GFP is highly expressed in cells carrying Cnp1-GFP under the *hht1*, *spd1*, and *spo12* promoter (Figure 7, B and C). Expression driven by these
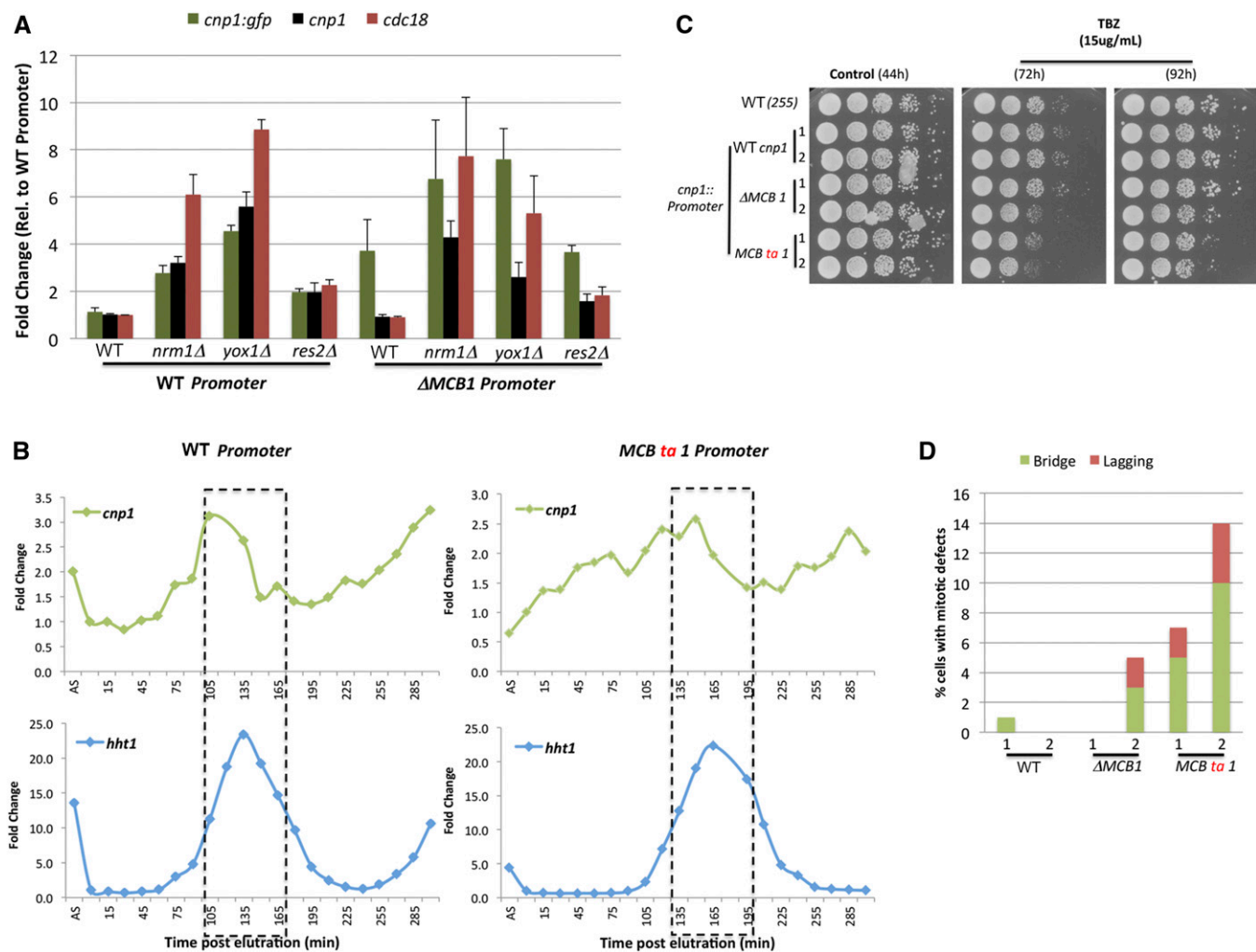
Figure 6 The MBF complex restricts CENP-A transcription to G1 phase. (A) Quantitative RT-PCR analysis of *cnp1* RNA levels in cells with a WT or ΔMCB1 *cnp1* promoter in combination with mutation of MBF genes. Cells carrying an extra copy of *cnp1* tagged with GFP under control of the WT or ΔMCB1 *cnp1* promoter were crossed with mutants for *nrm1*, *yox1*, or *res2* genes. Graph shows RNA fold changes for the *cnp1-gfp* transgene, endogenous *cnp1* and *cdc18* genes for the indicated genotypes. Fold change was calculated normalizing to levels in WT cells with the *cnp1-gfp* under the WT *cnp1* promoter. (B) *cnp1* and *hht1* mRNA levels measured by quantitative RT-PCR in synchronized cells with a WT or MCB1 box mutant promoter on *cnp1*. Dotted line indicates the time window when most of the cells are undergoing S phase, measured by the septation index. (C) TBZ sensitivity assays for Cnp1 promoter mutants. Serial dilutions of indicated strain cultures were plated onto YES medium supplemented with 15 μg/ml TBZ or control YES medium without TBZ. Pictures of colony growth were taken 72 or 96 hr postplating. (D) Overexpression of Cnp1-GFP causes chromosome segregation defects in MCB1 mutant cells. Cells were fixed and stained with DAPI staining. The percentage of mitotic cells showing bridged, and lagging chromosomes was quantified as in Figure 2C. MBF, MluI box-binding factors; MCB, MluI cell cycle box; TBZ, thiabendazole; WT, wild-type; YES, yeast extract with supplements.

promoters is higher compared to the *plo1* and *cdc15* promoters. These results indicate that the distribution pattern of CENP-A correlates with the strength of the promoters, rather than the timing of CENP-A expression for its association with centromeres. Consistent with this, a strain with *cnp1-gfp* under control of the *cdc18* promoter, which generates an ∼10-fold increase in *cnp1* mRNA (Figure 7B), exhibited ectopic localization of Cnp1-GFP. However, a second strain generated with the *cdc18* promoter showed only a fourfold increase in *cnp1* mRNA and displayed WT-like single foci Cnp1-GFP localization (data not shown). This result is especially interesting since the *cdc18* promoter drives expression at G1, the same timing as the *cnp1* promoter. The

previously reported mislocalization of CENP-A driven by the histone H3 promoter is likely due to overexpression rather than misregulation of the timing of CENP-A expression. This result suggests that tight cell cycle regulation of CENP-A transcription ensures that the proper level of CENP-A is generated.

Discussion

Cell cycle regulation of CENP-A transcription appears to be a universal feature across eukaryotes, but how transcription of CENP-A is regulated remains elusive. Here, we confirmed that CENP-A transcription in fission yeast peaks during G1 phase.
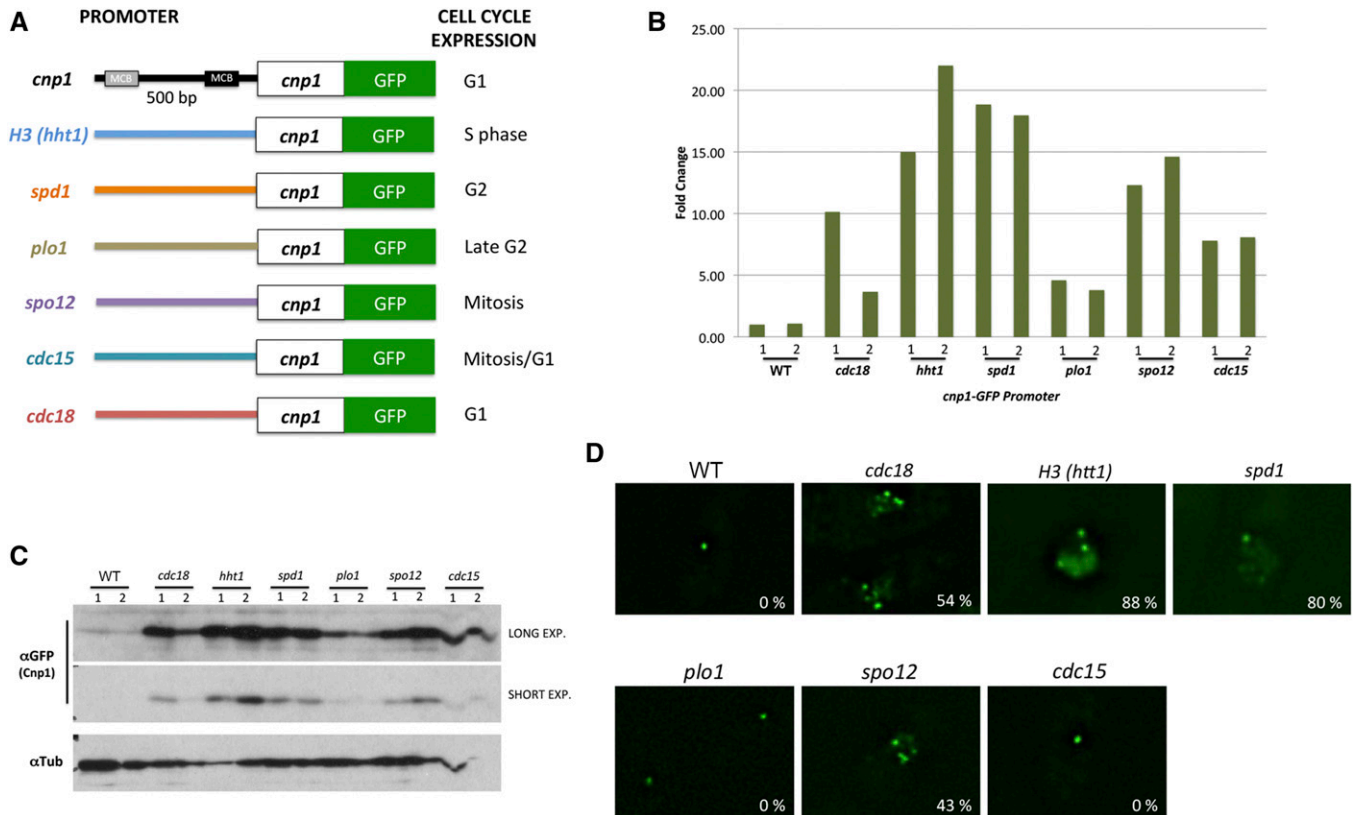
Figure 7 The timing of CENP-A expression is dispensable for its centromeric targeting. (A) Schematic diagram of the *cnp1-gfp* constructs under promoters that drive expression at different cell cycle stages. (B) Quantitative RT-PCR analysis of RNA levels of *cnp1-gfp* driven by different promoters. Graphic shows fold change compared to the WT *cnp1* promoter. (C) Western blotting analysis of Cnp1-GFP protein levels expressed by different promoters. Tubulin was used as a loading control. Short and long exposures are shown for anti-GFP blotting. (D) Distribution patterns of Cnp1-GFP expressed from different promoters. Percentage of cells showing multifoci phenotype is indicated for each sample. Exp., exposure; WT, wild-type.

We further identified components of the MBF complex, including Nrm1, Yox1, and Res2, that are required for cell cycle-dependent CENP-A transcription regulation. The MBF complex binds to the MCB motif in the CENP-A promoter to restrict its transcription to G1 phase (Figure 8). However, CENP-A can still target to centromeres when forced to express at non-G1 phase, indicating that timing of CENP-A transcription is not essential for its centromere localization. We conclude that cell cycle regulation of CENP-A transcription is a key control mechanism to ensure that the proper amount of CENP-A is generated across generations.

Using a visual genetic screen, we identified *nrm1Δ*, *yox1Δ*, and *res2Δ* mutants that exhibited excessive CENP-A-GFP and chromosome segregation defects. Nrm1, Yox1, and Res2 are components of the MBF complex, which regulates transcription during the G1/S transition of the cell cycle. We showed that CENP-A mRNA is significantly upregulated in *nrm1Δ* and *yox1Δ*, consistent with its role as a negative regulator of the MBF complex. Deletion of *res2* has a weaker effect on CENP-A transcription and chromosome segregation, likely resulting from the fact that Res2 has both negative and positive roles in MBF-mediated transcription. Cdc10, another component of the MBF complex, also has a dual role in regulating gene expression during G1/S (McInerny *et al.* 1995).

Accordingly, we found that CENP-A transcription is abnormal in *cdc10* mutant cells (Figure S2). Rep2 is considered to be the transcriptional activator of other MBF targets (Nakashima *et al.* 1995), but disruption of Rep2 does not have a strong effect on *cnp1* transcription. This suggests that Cnp1 regulation by the MBF proteins does not totally fit with the canonical regulation of the complex.

As expected, we found that the MBF complex binds to the promoter region of CENP-A. Mutations in the putative MBF-binding MCB motif −110-bp upstream of the start codon abolished the cell cycle transcription pattern of CENP-A, and resulted in its deregulated expression and a higher level of CENP-A transcripts, demonstrating that it is a *bona fide* MCB box. Disruption of the MCB box at its endogenous site gave rise to a cell cycle delay, TBZ sensitivity, and mitotic defects, indicative of chromosome missegregation. Our data suggest that the MBF repressors bind to the MCB box at the CENP-A promoter to restrict its expression to G1 phase, which prevents *cnp1* overexpression. The second putative MCB motif, localized at −475-bp upstream of the start codon appears not to be functional.

The level of CENP-A is tightly controlled. CENP-A overexpression leads to erroneous deposition of CENP-A to noncentromeric regions. This results in chromosome missegregation
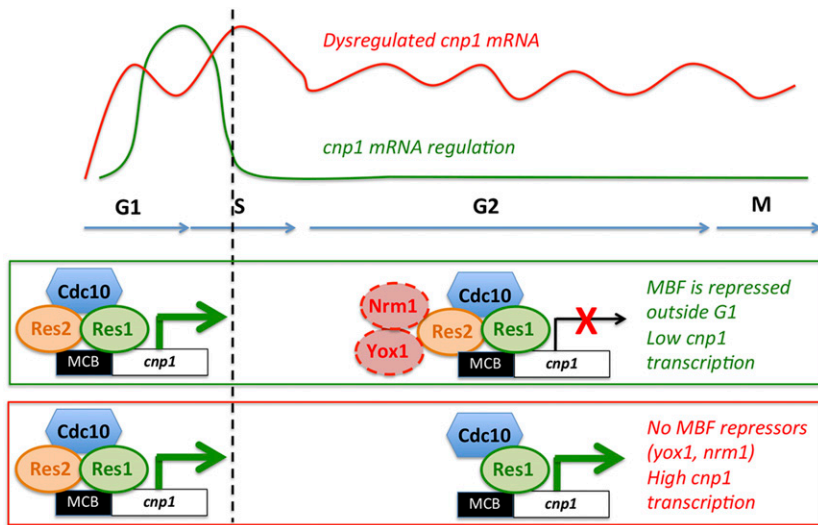
Figure 8 Model for cell cycle-regulated *cnp1* transcription by the MBF complex. During the G1/S transition, the MBF core complex (Cdc10, Res1, and Res2) binds to the MCB motif in the *cnp1* promoter to activate *cnp1* transcription. The MBF complex also induces the transcription of the *yox1* and *nrm1* genes, as well as other genes required for DNA replication. Yox1 and Nrm1 form a dimer and bind to the MBF core complex through interacting with Res2. The binding of Nrm1 and Yox1 inhibits the transcriptional induction activity of the complex, and establishes a negative feedback loop preventing the constitutive activation of *cnp1* for the rest of the cell cycle. In the absence of Nrm1 and Yox1, the MBF activator core complex remains active throughout the cell cycle, leading to an aberrant accumulation of *cnp1* transcripts. If the level of Cnp1 surpasses a certain threshold, the cell starts showing mitotic defects as a consequence of Cnp1 mislocalization. MBF, MluI box-binding factors; MCB, MluI cell cycle box.

and growth defects. Ubiquitin-dependent proteolysis has been shown to be a conserved post-translational mechanism to degrade excessive CENP-A (Collins *et al.* 2004; Moreno-Moreno *et al.* 2006; Hewawasam *et al.* 2010; Ranjitkar *et al.* 2010; Au *et al.* 2013; Gonzalez *et al.* 2014; Yang *et al.* 2018). This study demonstrates that transcriptional regulation of CENP-A is another important control mechanism to ensure that the proper amount of CENP-A is expressed. Disruption of the CENP-A transcription machinery also generates mistargeted CENP-A and chromosome segregation defects. Nevertheless, these mutants also show cell cycle deregulation of multiple genes required for S phase progression (Caetano *et al.* 2014). We cannot exclude the possibility that the observed mitotic phenotypes in the mutants could be, at least partially, due to replicative stress.

Interestingly, CENP-A transcription and the loading of CENP-A usually occur in different stages of the cell cycle. In fission yeast, Cnp1 is transcribed at G1, resulting in the protein pool increasing by approximately twofold during S phase. The increase in Cnp1 probably occurs in preparation for the next round of Cnp1 assembly that occurs in G2. The timing of CENP-A transcription is also often different from canonical histone transcription. It has been proposed that the restriction of histone gene transcription to S phase may prevent regular histones from competing with histone variants for incorporation into the chromosomes of nonreplicating cells (Bahler 2005). CENP-A in fission yeast is expressed at G1/S before histone transcription. How CENP-A is prevented from assembling into noncentromeric nucleosomes during replication is unclear. In addition to ubiquitin-dependent proteolysis, the nucleosome assembly protein (NAP) domain-containing Ccp1 and the chromatin remodeling complexes, such as facilitates chromatin transcription (FACT) and human histone cell cycle regulator (HIRA), also play important roles in removing mistargeted CENP-A (Choi *et al.* 2012; Deyter and Biggins 2014; Dong *et al.* 2016; Ciftci-Yilmaz *et al.* 2018). Perhaps these factors maintain the integrity of chromosome arms by excluding ectopic CENP-A during replication.

It has been shown that CENP-A expressed under the promoter of histone H3 in human cells is distributed throughout the nucleus. The observation led to the hypothesis that the timing of CENP-A expression acts as an important component of the CENP-A-targeting mechanism (Shelby *et al.* 1997, 2000). Our study also showed that cells expressing Cnp1 under the histone H3 promoter display excessive Cnp1-GFP foci with diffuse nuclear signal in fission yeast. However, Cnp1 driven by the *plo1* and *cdc15* promoters, which induce transcription at late G2 and mitosis/G1, respectively, can properly target to centromeres, indicating that the timing of CENP-A transcription is not absolutely required for its centromere localization. Consistent with this, deletion of the MCB1 box results in constitutive overexpression of CENP-A, but the protein is still assembled mostly at centromeres. Careful examination reveals that the distribution pattern of CENP-A driven by different promoters correlates with its expression level. Strong promoters, such as that of histone H3, lead to an abnormal distribution of CENP-A. On the other hand, CENP-A expressed from weaker promoters, including these of *plo1* and *cdc15*, still targets to centromeres. We noted that the expression levels expressed from the *plo1* and *cdc15* promoters are modestly higher than the level expressed by the native CENP-A promoter. These data are consistent with previous studies showing that when weakly overexpressed, CENP-A in fission yeast still associates specifically with centromeres (Choi *et al.* 2012; Gonzalez *et al.* 2014). Together, our results support our model that precise control of the timing of CENP-A transcription ensures that the proper level of CENP-A is expressed, rather than its targeting to centromeres.

Interestingly, we often observed significant variation in the level of Cnp1 expression in different clones carrying the same mutations of the MCB1 box in the endogenous *cnp1* promoter. Clones with higher Cnp1 overexpression exhibited increased TBZ sensitivity and mitotic defects. This result suggests that there may be a threshold of tolerance for Cnp1 overexpression, above which cells are strongly selected against. This may lead

to clonal variation by selecting cells that activate mechanisms preventing excessive Cnp1.

The MBF complex is functionally analogous to the E2F complex in plants and metazoans, which has been shown to control the G1/S and also G2/M transitions (Zhu *et al.* 2004; Bertoli *et al.* 2013). In *Arabidopsis*, E2fa binds to the promoter of CENP-A *in vivo*, and mutating the E2F-binding sites at the promoter results in increased reporter gene activity (Heckmann *et al.* 2011). Putative E2F-binding sites were also found in the human CENP-A promoter by an *in silico* study (Amato *et al.* 2009). Downregulation of E2F/RBR in human cells leads to increased RNA and protein levels of CENP-A (Sullivan *et al.* 2011). Thus, the mechanism underlying MBF-mediated transcriptional regulation of CENP-A expression may be conserved in plants and humans.

Literature Cited

Aligianni, S., D. H. Lackner, S. Klier, G. Rustici, B. T. Wilhelm *et al.*, 2009   The fission yeast homeodomain protein Yox1p binds to MBF and confines MBF-dependent cell-cycle transcription to G1-S via negative feedback. PLoS Genet. 5: e1000626. https://doi.org/10.1371/journal.pgen.1000626

Allshire, R. C., and G. H. Karpen, 2008   Epigenetic regulation of centromeric chromatin: old dogs, new tricks? Nat. Rev. Genet. 9: 923–937. https://doi.org/10.1038/nrg2466

Amato, A., T. Schillaci, L. Lentini, and A. Di Leonardo, 2009   CENPA overexpression promotes genome instability in pRb-depleted human cells. Mol. Cancer 8: 119.

Au, W. C., A. R. Dawson, D. W. Rawson, S. B. Taylor, R. E. Baker *et al.*, 2013   A novel role of the N terminus of budding yeast histone H3 variant Cse4 in ubiquitin-mediated proteolysis. Genetics 194: 513–518.

Ayté, J., J. F. Leis, A. Herrera, E. Tang, H. Yang *et al.*, 1995   The Schizosaccharomyces pombe MBF complex requires heterodimerization for entry into S phase. Mol. Cell. Biol. 15: 2589–2599. https://doi.org/10.1128/MCB.15.5.2589

Ayté, J., C. Schweitzer, P. Zarzov, P. Nurse, and J. A. DeCaprio, 2001   Feedback regulation of the MBF transcription factor by cyclin Cig2. Nat. Cell Biol. 3: 1043–1050.

Bahler, J., 2005   Cell-cycle control of gene expression in budding and fission yeast. Annu. Rev. Genet. 39: 69–94.

Bar-Joseph, Z., Z. Siegfried, M. Brandeis, B. Brors, Y. Lu *et al.*, 2008   Genome-wide transcriptional analysis of the human cell cycle identifies genes differentially regulated in normal and cancer cells. Proc. Natl. Acad. Sci. USA 105: 955–960.

Baum, B., J. Wuarin, and P. Nurse, 1997   Control of S-phase periodic transcription in the fission yeast mitotic cycle. EMBO J. 16: 4676–4688. https://doi.org/10.1093/emboj/16.15.4676

Bertoli, C., J. M. Skotheim, and R. A. de Bruin, 2013   Control of cell cycle transcription during G1 and S phases. Nat. Rev. Mol. Cell Biol. 14: 518–528. https://doi.org/10.1038/nrm3629

Black, B. E., and D. W. Cleveland, 2011   Epigenetic centromere propagation and the nature of CENP-a nucleosomes. Cell 144: 471–479.

Black, B. E., L. E. Jansen, P. S. Maddox, D. R. Foltz, A. B. Desai *et al.*, 2007   Centromere identity maintained by nucleosomes assembled with histone H3 containing the CENP-A targeting domain. Mol. Cell 25: 309–322. https://doi.org/10.1016/j.molcel.2006.12.018

Caetano, C., S. Klier, and R. A. de Bruin, 2011   Phosphorylation of the MBF repressor Yox1p by the DNA replication checkpoint keeps the G1/S cell-cycle transcriptional program active. PLoS One 6: e17211. https://doi.org/10.1371/journal.pone.0017211

Caetano, C., O. Limbo, S. Farmer, S. Klier, C. Dovey *et al.*, 2014   Tolerance of deregulated G1/S transcription depends on critical G1/S regulon genes to prevent catastrophic genome instability. Cell Rep. 9: 2279–2289. https://doi.org/10.1016/j.celrep.2014.11.039

Castillo, A. G., A. L. Pidoux, S. Catania, M. Durand-Dubief, E. S. Choi *et al.*, 2013   Telomeric repeats facilitate CENP-A(Cnp1) incorporation via telomere binding proteins. PLoS One 8: e69673 (erratum: Cell 8). https://doi.org/10.1371/journal.pone.0069673

Choi, E. S., A. Stralfors, S. Catania, A. G. Castillo, J. P. Svensson *et al.*, 2012   Factors that promote H3 chromatin integrity during transcription prevent promiscuous deposition of CENP-A (Cnp1) in fission yeast. PLoS Genet. 8: e1002985.

Ciftci-Yilmaz, S., W. C. Au, P. K. Mishra, J. R. Eisenstatt, J. Chang *et al.*, 2018   A genome-wide screen reveals a role for the HIR histone chaperone complex in preventing mislocalization of budding yeast CENP-A. Genetics 210: 203–218.

Collins, K. A., S. Furuyama, and S. Biggins, 2004   Proteolysis contributes to the exclusive centromere localization of the yeast Cse4/CENP-A histone H3 variant. Curr. Biol. 14: 1968–1972. https://doi.org/10.1016/j.cub.2004.10.024

de Bruin, R. A., T. I. Kalashnikova, C. Chahwan, W. H. McDonald, J. Wohlschlegel *et al.*, 2006   Constraining G1-specific transcription to late G1 phase: the MBF-associated corepressor Nrm1 acts via negative feedback. Mol. Cell 23: 483–496.

Deyter, G. M., and S. Biggins, 2014   The FACT complex interacts with the E3 ubiquitin ligase Psh1 to prevent ectopic localization of CENP-A. Genes Dev. 28: 1815–1826.

Dong, Q., F. X. Yin, F. Gao, Y. Shen, F. Zhang *et al.*, 2016   Ccp1 homodimer mediates chromatin integrity by antagonizing CENP-A loading. Mol. Cell 64: 79–91.

Dutta, C., P. K. Patel, A. Rosebrock, A. Oliva, J. Leatherwood *et al.*, 2008   The DNA replication checkpoint directly regulates MBF-dependent G1/S transcription. Mol. Cell. Biol. 28: 5977–5985. https://doi.org/10.1128/MCB.00596-08

Funabiki, H., I. Hagan, S. Uzawa, and M. Yanagida, 1993   Cell cycle-dependent specific positioning and clustering of centromeres and telomeres in fission yeast. J. Cell Biol. 121: 961–976. https://doi.org/10.1083/jcb.121.5.961

Gonzalez, M., H. He, S. Sun, C. Li, and F. Li, 2013   Cell cycle-dependent deposition of CENP-A requires the Dos1/2-Cdc20 complex. Proc. Natl. Acad. Sci. USA 110: 606–611.

Gonzalez, M., H. He, Q. Dong, S. Sun, and F. Li, 2014   Ectopic centromere nucleation by CENP-A in fission yeast. Genetics 198: 1433–1446. https://doi.org/10.1534/genetics.114.171173

Grant, G. D., L. Brooks, III, X. Zhang, J. M. Mahoney, V. Martyanov *et al.*, 2013   Identification of cell cycle-regulated genes periodically expressed in U2OS cells and their regulation by FOXM1 and E2F transcription factors. Mol. Biol. Cell 24: 3634–3650. https://doi.org/10.1091/mbc.e13-05-0264

Haase, S. B., and C. Wittenberg, 2014   Topology and control of the cell-cycle-regulated transcriptional circuitry. Genetics 196: 65–90. https://doi.org/10.1534/genetics.113.152595

He, H., S. Zhang, D. Wang, A. Hochwagen, and F. Li, 2016   Condensin promotes position effects within tandem DNA repeats via the RITS complex. Cell Rep. 14: 1018–1024. https://doi.org/10.1016/j.celrep.2016.01.006

He, H., Y. Li, Q. Dong, A. Y. Chang, F. Gao et al., 2017   Coordinated regulation of heterochromatin inheritance by Dpb3-Dpb4 complex. Proc. Natl. Acad. Sci. USA 114: 12524–12529. https://doi.org/10.1073/pnas.1712961114

Heckmann, S., I. Lermontova, B. Berckmans, L. De Veylder, H. Baumlein et al., 2011   The E2F transcription factor family regulates CENH3 expression in Arabidopsis thaliana. Plant J. 68: 646–656. https://doi.org/10.1111/j.1365-313X.2011.04715.x

Heun, P., S. Erhardt, M. D. Blower, S. Weiss, A. D. Skora et al., 2006   Mislocalization of the Drosophila centromere-specific histone CID promotes formation of functional ectopic kinetochores. Dev. Cell 10: 303–315. https://doi.org/10.1016/j.devcel.2006.01.014

Hewawasam, G., M. Shivaraju, M. Mattingly, S. Venkatesh, S. Martin-Brown et al., 2010   Psh1 is an E3 ubiquitin ligase that targets the centromeric histone variant Cse4. Mol. Cell 40: 444–454. https://doi.org/10.1016/j.molcel.2010.10.014

Huang, T., P. Zhang, W. Li, T. Zhao, Z. Zhang et al., 2017   G9A promotes tumor cell growth and invasion by silencing CASP1 in non-small-cell lung cancer cells. Cell Death Dis. 8: e2726. https://doi.org/10.1038/cddis.2017.65

Jansen, L. E., B. E. Black, D. R. Foltz, and D. W. Cleveland, 2007   Propagation of centromeric chromatin requires exit from mitosis. J. Cell Biol. 176: 795–805. https://doi.org/10.1083/jcb.200701066

Kelly, T. J., G. S. Martin, S. L. Forsburg, R. J. Stephen, A. Russo et al., 1993   The fission yeast cdc18+ gene product couples S phase to START and mitosis. Cell 74: 371–382. https://doi.org/10.1016/0092-8674(93)90427-R

Kong, L., P. Zhang, W. Li, Y. Yang, Y. Tian et al., 2016   KDM1A promotes tumor cell invasion by silencing TIMP3 in non-small cell lung cancer cells. Oncotarget 7: 27959–27974.

Lando, D., U. Endesfelder, H. Berger, L. Subramanian, P. D. Dunne et al., 2012   Quantitative single-molecule microscopy reveals that CENP-A(Cnp1) deposition occurs during G2 in fission yeast. Open Biol. 2: 120078. https://doi.org/10.1098/rsob.120078

Lermontova, I., V. Schubert, J. Fuchs, S. Klatte, J. Macas et al., 2006   Loading of Arabidopsis centromeric histone CENH3 occurs mainly during G2 and requires the presence of the histone fold domain. Plant Cell 18: 2443–2451. https://doi.org/10.1105/tpc.106.043174

Li, Y. M., X. H. Liu, X. Z. Cao, L. Wang, and M. H. Zhu, 2007   Expression of centromere protein A in hepatocellular carcinoma. Zhonghua Bing Li Xue Za Zhi 36: 175–178.

Lowndes, N. F., C. J. McInerny, A. L. Johnson, P. A. Fantes, and L. H. Johnston, 1992   Control of DNA synthesis genes in fission yeast by the cell-cycle gene cdc10+. Nature 355: 449–453. https://doi.org/10.1038/355449a0

McInerny, C. J., P. J. Kersey, J. Creanor, and P. A. Fantes, 1995   Positive and negative roles for cdc10 in cell cycle gene expression. Nucleic Acids Res. 23: 4761–4768. https://doi.org/10.1093/nar/23.23.4761

McKinley, K. L., and I. M. Cheeseman, 2016   The molecular basis for centromere identity and function. Nat. Rev. Mol. Cell Biol. 17: 16–29. https://doi.org/10.1038/nrm.2015.5

Mellone, B. G., K. J. Grive, V. Shteyn, S. R. Bowers, I. Oderberg et al., 2011   Assembly of Drosophila centromeric chromatin proteins during mitosis. PLoS Genet. 7: e1002068. https://doi.org/10.1371/journal.pgen.1002068

Moreno, S., A. Klar, and P. Nurse, 1991   Molecular genetic analysis of fission yeast Schizosaccharomyces pombe. Methods Enzymol. 194: 795–823. https://doi.org/10.1016/0076-6879(91)94059-L

Moreno-Moreno, O., M. Torras-Llort, and F. Azorin, 2006   Proteolysis restricts localization of CID, the centromere-specific histone H3 variant of Drosophila, to centromeres. Nucleic Acids Res. 34: 6247–6255. https://doi.org/10.1093/nar/gkl902

Nakashima, N., K. Tanaka, S. Sturm, and H. Okayama, 1995   Fission yeast Rep2 is a putative transcriptional activator subunit for the cell cycle 'start' function of Res2-Cdc10. EMBO J. 14: 4794–4802. https://doi.org/10.1002/j.1460-2075.1995.tb00161.x

Olszak, A. M., D. van Essen, A. J. Pereira, S. Diehl, T. Manke et al., 2011   Heterochromatin boundaries are hotspots for de novo kinetochore formation. Nat. Cell Biol. 13: 799–808. https://doi.org/10.1038/ncb2272

Pearson, C. G., E. Yeh, M. Gardner, D. Odde, E. D. Salmon et al., 2004   Stable kinetochore-microtubule attachment constrains centromere positioning in metaphase. Curr. Biol. 14: 1962–1967. https://doi.org/10.1016/j.cub.2004.09.086

Purtill, F. S., S. K. Whitehall, E. S. Williams, C. J. McInerny, A. D. Sharrocks et al., 2011   A homeodomain transcription factor regulates the DNA replication checkpoint in yeast. Cell Cycle 10: 664–670. https://doi.org/10.4161/cc.10.4.14824

Ranjitkar, P., M. O. Press, X. Yi, R. Baker, M. J. MacCoss et al., 2010   An E3 ubiquitin ligase prevents ectopic localization of the centromeric histone H3 variant via the centromere targeting domain. Mol. Cell 40: 455–464. https://doi.org/10.1016/j.molcel.2010.09.025

Rattray, A. M., and B. Muller, 2012   The control of histone gene expression. Biochem. Soc. Trans. 40: 880–885. https://doi.org/10.1042/BST20120065

Rustici, G., J. Mata, K. Kivinen, P. Lio, C. J. Penkett et al., 2004   Periodic gene expression program of the fission yeast cell cycle. Nat. Genet. 36: 809–817. https://doi.org/10.1038/ng1377

Schuh, M., C. F. Lehner, and S. Heidmann, 2007   Incorporation of Drosophila CID/CENP-A and CENP-C into centromeres during early embryonic anaphase. Curr. Biol. 17: 237–243. https://doi.org/10.1016/j.cub.2006.11.051

Scott, K. C., and B. A. Sullivan, 2014   Neocentromeres: a place for everything and everything in its place. Trends Genet. 30: 66–74. https://doi.org/10.1016/j.tig.2013.11.003

Shelby, R. D., O. Vafa, and K. F. Sullivan, 1997   Assembly of CENP-A into centromeric chromatin requires a cooperative array of nucleosomal DNA contact sites. J. Cell Biol. 136: 501–513. https://doi.org/10.1083/jcb.136.3.501

Shelby, R. D., K. Monier, and K. F. Sullivan, 2000   Chromatin assembly at kinetochores is uncoupled from DNA replication. J. Cell Biol. 151: 1113–1118. https://doi.org/10.1083/jcb.151.5.1113

Shrestha, R. L., G. S. Ahn, M. I. Staples, K. M. Sathyan, T. S. Karpova et al., 2017   Mislocalization of centromeric histone H3 variant CENP-A contributes to chromosomal instability (CIN) in human cells. Oncotarget 8: 46781–46800. https://doi.org/10.18632/oncotarget.18108

Sullivan, L. L., C. D. Boivin, B. Mravinac, I. Y. Song, and B. A. Sullivan, 2011   Genomic size of CENP-A domain is proportional to total alpha satellite array size at human centromeres and expands in cancer cells. Chromosome Res. 19: 457–470. https://doi.org/10.1007/s10577-011-9208-5

Takahashi, K., E. S. Chen, and M. Yanagida, 2000   Requirement of Mis6 centromere connector for localizing a CENP-A-like protein in fission yeast. Science 288: 2215–2219. https://doi.org/10.1126/science.288.5474.2215

Takayama, Y., and K. Takahashi, 2007   Differential regulation of repeated histone genes during the fission yeast cell cycle.

Nucleic Acids Res. 35: 3223–3237. https://doi.org/10.1093/nar/gkm213

Takayama, Y., H. Sato, S. Saitoh, Y. Ogiyama, F. Masuda *et al.*, 2008 Biphasic incorporation of centromeric histone CENP-A in fission yeast. Mol. Biol. Cell 19: 682–690. https://doi.org/10.1091/mbc.e07-05-0504

Tomonaga, T., K. Matsushita, S. Yamaguchi, T. Oohashi, H. Shimada *et al.*, 2003 Overexpression and mistargeting of centromere protein-A in human primary colorectal cancer. Cancer Res. 63: 3511–3516.

Tormos-Pérez, M., L. Pérez-Hidalgo, and S. Moreno, 2016 Fission yeast cell cycle synchronization methods. Methods Mol. Biol. 1369: 293–308. https://doi.org/10.1007/978-1-4939-3145-3_20

Whitehall, S., P. Stacey, K. Dawson, and N. Jones, 1999 Cell cycle-regulated transcription in fission yeast: Cdc10-Res protein interactions during the cell cycle and domains required for regulated transcription. Mol. Biol. Cell 10: 3705–3715. https://doi.org/10.1091/mbc.10.11.3705

Whitfield, M. L., G. Sherlock, A. J. Saldanha, J. I. Murray, C. A. Ball *et al.*, 2002 Identification of genes periodically expressed in the human cell cycle and their expression in tumors. Mol. Biol. Cell 13: 1977–2000. https://doi.org/10.1091/mbc.02-02-0030

Wisniewski, J., B. Hajj, J. Chen, G. Mizuguchi, H. Xiao *et al.*, 2014 Imaging the fate of histone Cse4 reveals de novo replacement in S phase and subsequent stable residence at centromeres. Elife 3: e02203. https://doi.org/10.7554/eLife.02203

Yang, J., and F. Li, 2018 In situ chromatin-binding assay using epifluorescent microscopy in S. pombe. Methods Mol. Biol. 1721: 155–165. https://doi.org/10.1007/978-1-4939-7546-4_14

Yang, J., S. Sun, S. Zhang, M. Gonzalez, Q. Dong *et al.*, 2018 Heterochromatin and RNAi regulate centromeres by protecting CENP-A from ubiquitin-mediated degradation. PLoS Genet. 14: e1007572. https://doi.org/10.1371/journal.pgen.1007572

Zhang, W., J. H. Mao, W. Zhu, A. K. Jain, K. Liu *et al.*, 2016 Centromere and kinetochore gene misexpression predicts cancer patient survival and response to radiotherapy and chemotherapy. Nat. Commun. 7: 12619. https://doi.org/10.1038/ncomms12619

Zhu, W., P. H. Giangrande, and J. R. Nevins, 2004 E2Fs link the control of G1/S and G2/M transcription. EMBO J. 23: 4615–4626. https://doi.org/10.1038/sj.emboj.7600459

Zhu, Y., T. Takeda, S. Whitehall, N. Peat, and N. Jones, 1997 Functional characterization of the fission yeast Start-specific transcription factor Res2. EMBO J. 16: 1023–1034. https://doi.org/10.1093/emboj/16.5.1023

Communicating editor: M. Freitag